Design and optimization of an IPMSM with fixed outer dimensions for application in HEVs

Thomas Finken
Institute of Electrical Machines
RWTH Aachen University
Schinkelstr. 4, 52056 Aachen, Germany
Email: thomas.finken@iem.rwth-aachen.de

Kay Hameyer
Institute of Electrical Machines
RWTH Aachen University
Schinkelstr. 4, 52056 Aachen, Germany
Email: kay.hameyer@iem.rwth-aachen.de

***Abstract*—Permanent magnet excited synchronous machines (PMSM) are finding more and more applications nowadays. They are particularly well adapted when a high power to volume ratio or a high overall efficiency are required. This is in particular the case for hybrid electric vehicles (HEV), due to the limited space available in drive trains and the severe constraints on fuel consumption. PM-motors are therefore the most widespread machine type in parallel HEVs. This paper presents the design and optimization of an internal PM-motor (IPMSM) under the constraint that the outer dimensions of the machine are fixed. The optimal rotor radius and the appropriate pole pair number of the machine are determined by means of analytical calculations and finite element (FE) simulations. A geometry optimization is performed, considering all losses (i.e. copper-, iron- and eddy-current losses), as well as the demagnetization resistance and the effect of centrifugal forces at high rotational speeds. In order to determine the field weakening capability and to generate the speed-torque as well as the speed-power characteristics, the direct- and quadrature-axis inductances are calculated in function of the load current and the field weakening angle.**

I. Introduction

An increasing awareness on ecological issues and the fossil-fuel shortage are strong incentives to develop more efficient vehicles, with lower fuel consumption but without reducing driving comfort. The hybrid electric vehicle (HEV), which combines the drive power of an internal combustion engine (ICE) and that of one or several electrical machines (EM), is a promising concept in this regard.

According to the pursued hybrid concept, the applied electrical machine has to be optimized for a range of operating points. Besides the fast start/stop function, it must also operate as a generator, as support traction in the so called boost operation, as a drive during electrical traction, as well as an electrodynamic brake for recuperation. In addition to the specifications on torque and speed resulting from named functionality, the main demands are: a high overall efficiency within a large range of the torque-speed characteristic, a high overload capacity, small installation space and weight, and a high reliability at low costs. With such requirements in power, efficiency, installation space and weight, the design of the machines is particularly challenging. According to several comparative studies in papers, reports or surveys like [1]- [5] and to an earlier work by this author [6], the PMSM appears to be the most suitable electrical machine for parallel hybrid systems, because of its high power density and its good overall efficiency in a wide speed range.

Within the scope of the BMWi [1] cooperative project *Europa Hybrid* [7], an IPMSM is developed for a parallel hybrid electric vehicle. In this paper a design and optimization approach for an IPMSM with fixed outer dimensions is presented. Starting with an analytical consideration and moreover with FE simulations, the degrees of freedom such as the rotor radius and the pole pair number are determined according to the machine requirements. Furthermore geometry-optimization steps are performed to improve the machine's power and overall efficiency.

II. Initial design

Electrical machines are usually dimensioned by means of analytical formulas. In particular, the stator diameter is directly derived from the value of the nominal power [8], [9]. But if the available installation space is limited and the outer dimensions are fixed, the approach must be different. In this case the rotor diameter D is a degree of freedom and the stator diameter D_S constant. A given force produces a torque that is proportional to the radius, i.e. the torque is at least linearly proportional to the diameter. Moreover, if the diameter increases, there is more room for magnets around the rotor which increases the specific magnetic loading. Therefore, torque and thus power increase with the diameter. But increasing the rotor diameter lowers the area of the stator. The area available for current injection decreases then, and if a constant current density is assumed, the specific electric loading A decreases as well. As a result, a maximum of the torque can be expected for an intermediate value of the rotor diameter D.

From analytical considerations (see Fig. 1), the tangential force F_α can be calculated from the air-gap field by the means of Maxwell Stress Tensor:

$$F_\alpha = \oint_F B_n H_t dF = \frac{lD}{2} \oint_0^{2\pi} B_n H_t d\alpha. \tag{1}$$

[1] Bundesministerium für Wirtschaft und Technologie (German Federal Ministry of Economics and Technology)

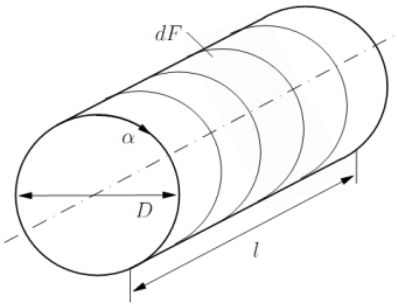

Fig. 1. Geometrical values of the stator bore.

With the simplification $B_n = B(\alpha)$ and $H_t = \frac{I}{l} = A(\alpha)$, the torque T is given by:

$$T = \frac{D}{2} F_\alpha = \frac{lD^2}{4} \oint_0^{2\pi} B(\alpha) A(\alpha) d\alpha. \tag{2}$$

The specific electric loading A is proportional to the stator area available for current injection and to the current density J:

$$A \sim \frac{I_{tot}}{\pi D} \sim \frac{J}{\pi D} \left[\pi \left(\frac{D_S}{2} \right)^2 - \pi \left(\frac{D}{2} \right)^2 \right]. \tag{3}$$

Therefore, the torque is proportional to:

$$T \sim D^3 \left(\frac{D_S^2}{D^2} - 1 \right) = D \cdot D_S^2 - D^3. \tag{4}$$

If the fixed outer diameter is $D_S = 146$mm, the normalized torque reaches a maximum at about $D = 84$mm, as depicted in Fig. 2.

Another degree of freedom is the pole pair number p, which influences the rotor size and thus the volume of a machine when using analytical formulas - increasing the poles increases the force generated by the motor. Furthermore, the stator-yoke height and the length of the end winding take up less space with increasing pole pair number. With a decreasing volume at constant power, the power density increases. However, increasing the number of poles implies decreasing the magnet width and enlarging the relative amount of magnet leakage flux, which in turn reduces the air gap flux density. So the force will not increase indefinitely but will actually decrease with a further increase of the magnet poles. Thus there exist an optimum number of magnet poles.

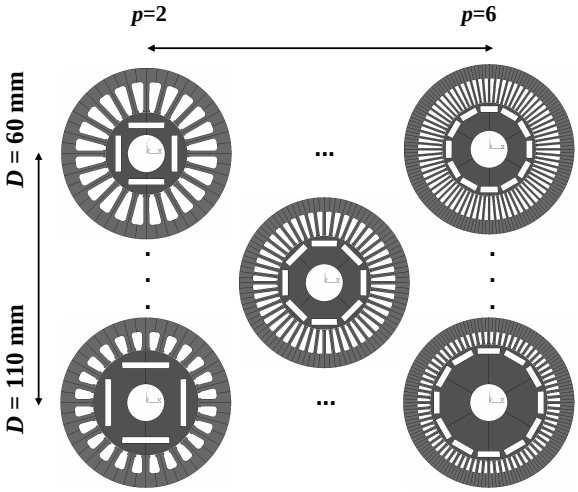

Fig. 3. The matrix of D- and p-variations.

Moreover, iron losses increase more than proportional with frequency, and the higher the pole pair number the higher the frequency of the stator currents and of the alternating magnetic field. The iron losses are the dominant losses in PMSMs at high rotational speeds. So the total losses increase significantly with increasing pole number at this speed range and thus the overall efficiency decreases.

Since the effect of the pole pair number can not be determined accurately by analytical formulae (due to named effects of flux leakage and iron losses), numerical FE simulations are performed. A matrix of geometry variations (see Fig. 3) $[p = 2..6, D = 60..110\text{mm}]$ is established in order to study the effect of pole pair variation, as well as to verify the analytical estimation of optimal rotor diameter.

This analysis is performed on several stator types, one with

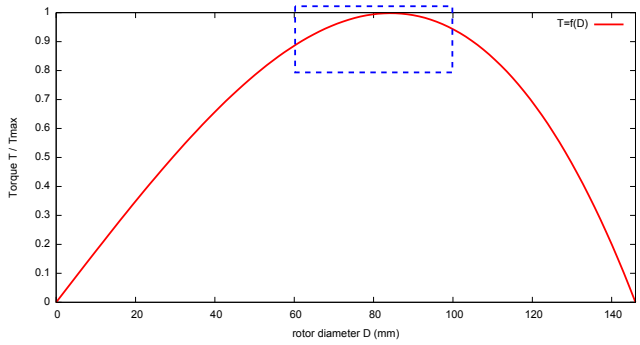

Fig. 2. The normalized torque depending on the rotor diameter.

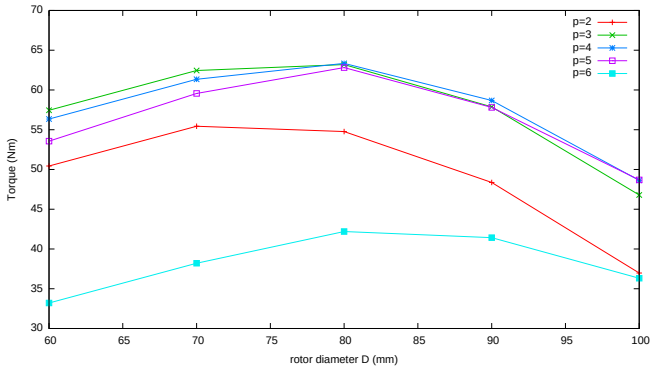

Fig. 4. Numerical calculated torque.

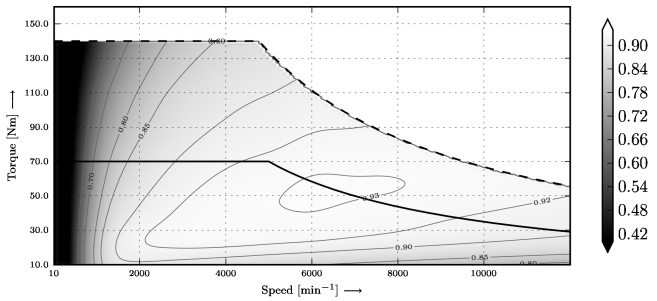

(a) p=3

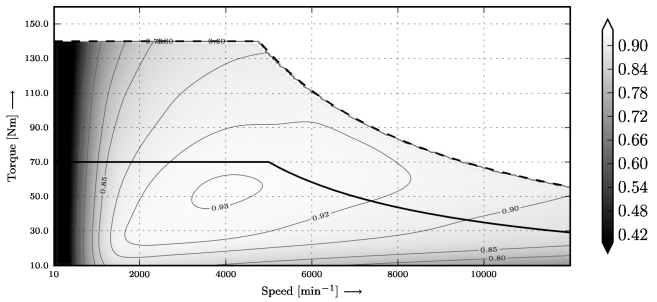

(b) p=4

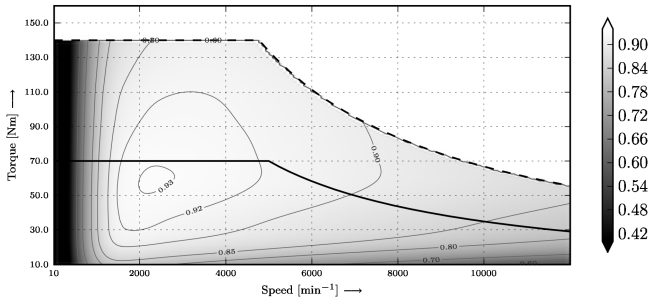

(c) p=5

Fig. 5. Efficiency maps depending on the pole-pair number.

a concentrated winding and two with distributed windings and different slot/pole ratio and short-pitching ($q = 2$ and $q = 1.5$). The following parameters remain constant for all geometries: the axial active length $l = 224$mm, the outer stator diameter $D_S = 146$mm and an air gap of $\delta = 0.7$mm. The nominal current density in the copper was set to the maximum allowed in an air-cooled machine, i.e. $J_n = 6$A/mm^2, and the copper space factor to $k_{cu} = 0.6$.

The simulation results with the distributed-winding are, as an example, depicted in Fig. 4. The maximum average torque depending on the rotor diameter has, in agreement with the analytical estimation, its maximum at $D = 80$mm. The pole pair numbers $3 \leq p \leq 5$ nearly provide the same torque. However, with increasing p the torque/current ratio is improved and thus the copper losses of the stator windings are lowered; on the other hand the iron losses increase with the pole pair number. This means, the losses can be moved into the stator by reducing the pole pair number, which make them easier to dissipate. In this case, copper losses are increased in

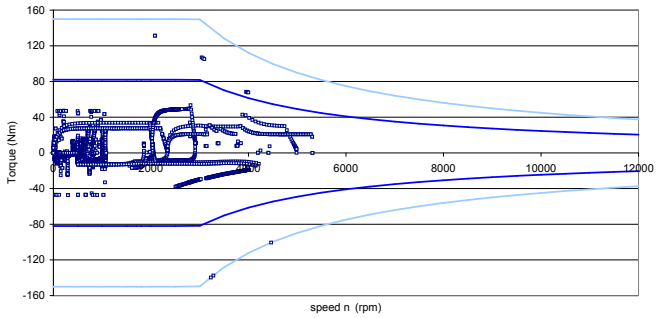

Fig. 6. Exemplary frequency distribution for a parallel HEV.

the stator and iron losses on the whole, and therefore rotor losses, are reduced. In addition, the range of high efficiency can be moved either to low rotational speeds (high p) or to high speeds (low p). In Fig. 5 the efficiency maps for the pole pair numbers $3 \leq p \leq 5$ are depicted to illustrate the above-named interrelation (the pole-number variation was performed with the final and optimized machine design). The efficiency maps for motor operation are calculated as described in the following section.

How far the reduction of p is reasonable depends on the required speed range, according to the frequency distribution of the operating points during a drive cycle. These frequency distributions are required to achieve an optimized machine design, which fulfills the vehicle's demands, and are determined by vehicle simulations. The vehicle-simulation model, describing a parallel HEV, includes the combustion engine, the transmission, the vehicle data, a battery and the electrical machine. Depending on the control strategy and the drive cycle, the frequency distribution of the expected operation points of the electrical machine can be determined - in Fig. 6 an exemplary frequency distribution (motor and generator operation) is depicted for a parallel HEV and an extra-urban drive cycle. The electrical machine must be designed in such a way that the range of best efficiency meets the range of most frequent operation points, i.e. the average overall efficiency must be maximized in order to improve the energy balance and reduce the vehicle's fuel consumption.

A good compromise in this case is the pole pair number of $p = 4$, examined drive cycles are an intra-urban, an extra-urban, a highway and a start drive cycle. The rotor diameter is chosen to $D = 80$mm.

III. Geometry Optimization

Following the initial design, the geometry optimization is performed. The final geometry is obtained in several steps (see Fig. 7) optimizing the rotor diameter, pole pitch, magnet height, tooth width, yoke height, addendum and the tooth tip width.

The properties of the machine are calculated to determine the effect for each geometry variation. The induced voltage, calculated at no-load operation, depends on the winding design and has to fulfill following safety condition: the induced voltage at maximum rotational speed must not exceed a defined

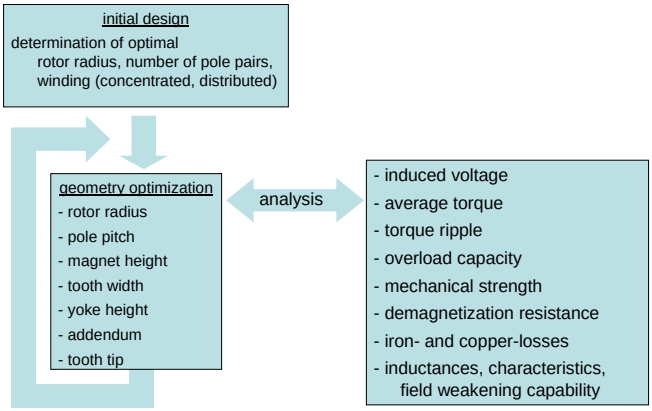

Fig. 7. Iterative optimization approach.

voltage limit, to avoid damage at the power electronics in case of control failure and missing field weakening capability.

In order to determine the mechanical output power, the average torque, as a function of the field weakening angle, and the torque ripple are calculated. The overload capacity is determined by checking the dependency of the demagnetization resistance on the load current.

Since the efficiency of the machine has to be optimized, the iron- and copper losses are also calculated. The calculation of the iron losses is performed by quasi-static numerical FE simulations and an improved post-processing formula based on the loss separation principle [10]- [11], which takes into account the skin effect of the eddy currents in the steel sheet and the effect of the flux distortion onto the hysteresis losses. The eddy current losses of the magnets are determined by transient 3D simulations. To calculate the copper losses, the winding resistances are determined depending on the number of turns and winding geometry. The mechanical losses are estimated by a percentage factor of the mechanical output power. Since the losses must be known for all operation points, they are calculated depending on the load current ($I = k \cdot I_n$ with k = 0.1, 0.25, 0.5, 1.0, 1.5, 2.5, 3.0), the field weakening angle ($\psi = -90°...90°$) and the speed ($n = 10...12000\text{min}^{-1}$).

By means of the flux linkage method [12] the direct- and quadrature-axis inductances (L_d and L_q, see Fig. 8(a)) are calculated as a function of the load current ($I = k \cdot I_n$ with k = 0.5, 1.0, 1.5, 2.5) and the field weakening angle ($\psi = -90°..90°$) as well as the differential inductances (L_{dd} and L_{qq}). The inductances L_d and L_q are required to determine the field weakening capability and to determine the torque for each operation point by the torque equation based on the fundamental-wave model of the synchronous machine:

$$T = \frac{3p}{\omega} \cdot [U_p - I_d \cdot (X_q - X_d)] \cdot I_q \qquad (5)$$

This analytical formula, combined with the voltage equation, provides a fast way to generate the speed-torque and the speed-power characteristics, which are limited by maximum

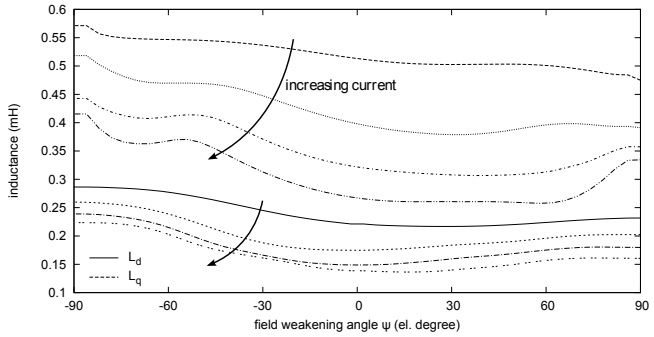

(a) L_d and L_q depending on current and field weakening angle ψ.

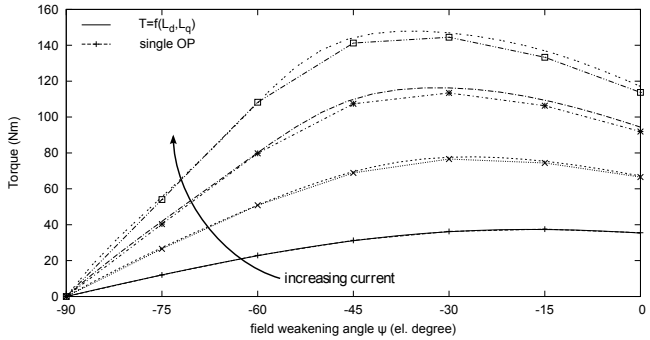

(b) Torque depending on current and field weakening angle ψ.

Fig. 8. Characteristics of inductances and torque.

voltage and maximum current. A comparison of the torque calculated by the fundamental-wave equation and the numerically calculated torque for each operation point is depicted in Fig. 8(b). The inductances L_{dd} and L_{qq} are required to permit a fast control model.

The speed-torque characteristics in combination with computed losses and efficiencies allows to generate efficiency maps and losses maps, which are essential to determine thermal operation limits and to design the machine's cooling.

A. Design of the embedded permanent magnets

The machine is operated with speeds up to 12,000min^{-1} causing considerable material stress at the rotor. For this reason (and for an improved overload capacity) the permanent magnets are buried in the studied machine. However, there is a disadvantage. Since the magnets are entirely surrounded by ferromagnetic steel, the main part of the magnetic flux may

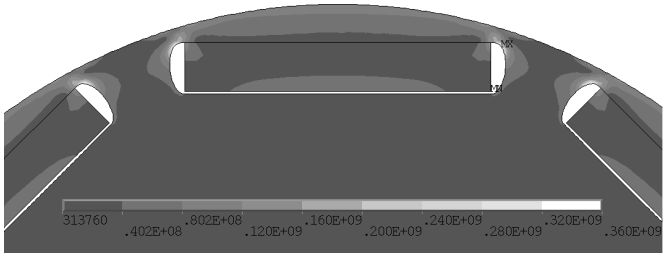

Fig. 9. Mechanical stress at high rotational speeds.

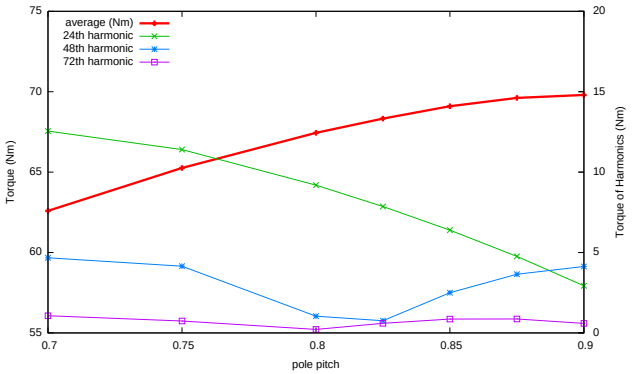

Fig. 10. The variation of the pole-pitch ratio.

close in the rotor - a magnetic short circuit. This flux neither cross the air gap nor the stator coils and it is not available for voltage induction and torque generation.

To avoid this effect, the bridges over the buried permanent magnets have to be as thin as possible to reduce the area, available for the magnetic short-circuit. As the saturation of this area increases, the magnetic resistance via air gap and stator will relatively decrease and a larger part of the magnetic flux will accordingly close through air-gap and rotor. But the remaining permanent-magnet fixation must assure sufficient mechanical strength at high speed. A compromise between sufficient mechanical strength and efficient permanent-magnet use has to be found. Therefore, the mechanical stress was calculated for all rotor configurations to validate a sufficient mechanical strength provided by the bridges, fixing the magnets inside the rotor (see Fig. 9).

B. Variation of the pole-pitch ratio

The design of the electrical machine must afford a high power density and therefore a high torque. Due to its integration into the driveline of the parallel HEV, the machine must have a low torque ripple and cogging torque as well. The pole pitch affects all these properties. The higher the pole-pitch ratio the wider the permanent magnets, i.e. the magnetic air-gap flux increase and thus the torque. But the pole-pitch ratio also affects the shape of the air-gap flux and the induced voltage: with a decreasing pole pitch the induced voltage becomes more sinusoidal, which reduces the torque ripple [13]. But the torque ripple also depends on the interaction of tooth width and pole pitch; this interaction can be calculated by numerical torque calculations. To determine the effect of a varying pole-pitch ratio and to optimize both the average torque and the torque ripple, several calculations were performed - the result is depicted in Fig. 10. The pole-pitch ratio is chosen to 82.5%. In that point the average torque is near to saturation so a further increase of the pole pitch hardly provides an improvement of the torque. In addition there is a local minimum of the 2nd harmonic of the torque ripple (48th harmonic of the fundamental speed).

C. The magnet height

During the initial design the magnet height is estimated by analytical formulas depending on the machine's dimensions, the magnet's demagnetization curve and the specified value of the air-gap flux density. Since the rare-earth magnets are an important price determinant, the dimension of the magnets must be optimized. Increasing the magnet height increases the magnetic flux and thus the induced voltage and torque. However, these values will not increase indefinitely due to the saturation of the iron lamination. Therefore, limiting the magnet height to a value near saturation, leads to a good compromise between the resulting torque and costs. To protect the magnets from demagnetization, the demagnetization capability is computed for each studied magnet height depending on the load current and temperature. The chosen height of the magnets provides a sufficient demagnetization capability up to both the maximum load current provided by the power electronics and the maximum expected temperature.

D. The variation of the tooth-tip width

Many machines nowadays use pre-formed windings providing a high copper-fill factor and a good cooling ability due to its well-arranged end windings. These pre-formed windings are usually slipped onto the tooth, so teeth without tooth tips are required. However, missing tooth tips increase the torque ripple and the rotor flux leakage. Furthermore tooth tips reduce the variation in air gap permeance as a function of position, thereby reducing cogging torque. But on the other hand an increasing width of the tooth tips increases the slot leakage inductance. Hence a tradeoff and an optimum tooth-tip width exist.

In Fig. 11(a) the result of a varying tooth-tip width is illustrated - a slot to tooth tip ratio of 1 means no tooth tips, the tooth-tip width is increasing with a decreasing ratio. A local maximum of the average torque exists at the ratio of 0.5. The torque ripple increases with decreasing tooth tip, as mentioned before.

Apart from that, iron losses are decreasing in the rotor (see Fig. 11(b)) and increasing in the stator (see Fig. 11(c)) with increasing tooth tip (total iron losses remains approximately constant), i.e. the iron losses can be moved from rotor to the stator. This is a great advantage because the permanent magnets are protected from heating and the heat, caused by the losses, can be dissipated more easily. Hence, the stator is designed with tooth tips. To keep named advantages of both the pre-formed windings and the tooth tips, the winding is a pre-formed winding, which is inserted from one side and soldered at the other side.

E. Further geometry variations

Further optimization steps include a variation of the tooth width, the yoke height and the addendum. Increasing the tooth width or the yoke height for example reduces the magnetic saturation and therefore decreases the iron losses. However, increasing the tooth width or the yoke height decreases the area available for the stator winding, which in turn decreases either

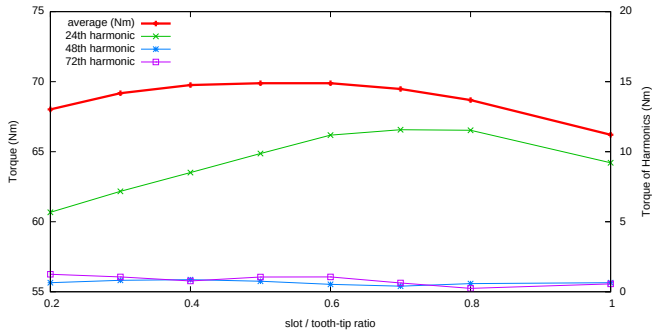

(a) average torque and torque rippel

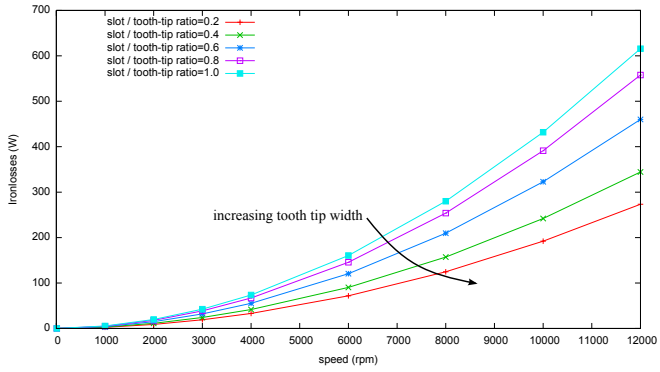

(b) rotor iron losses

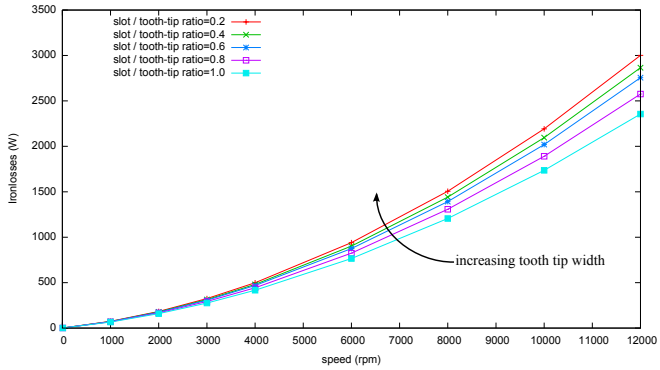

(c) stator iron losses

Fig. 11. The variation of the tooth-tip width.

the torque (if keeping the current density constant) or increases the losses (if keeping the current constant). So a compromise between maximum torque and minimum losses has to be found. To achieve a good exploitation and simultaneously keep the losses low, the named geometry parameters were designed in that way, that the resulting electrical properties are either in a local maximum or near saturation without operating the machine's lamination in magnetic saturation.

The resulting dimensions and values of the final geometry are listed in Table I.

IV. Conclusion

With regard to the restricted installation space in the drive train of an HEV, an approach to design and optimize an IPMSM with fixed outer dimensions is presented in this paper.

TABLE I
THE FINAL MACHINE DESIGN AND DATA.

rated power	35 kW	pole-pair number	4
max. power	70 kW	active length	224 mm
rated speed	5000 min^{-1}	stator diameter	146 mm
max. speed	12000 min^{-1}	rotor diameter	92 mm
DC link voltage	650 V	air gap	0.7 mm
rated current	60 A	shaft diameter	50 mm
max. efficiency	93%	magnet dimensions	25x4 mm^2

Electrical machines are usually dimensioned by means of analytical formulas. In particular, the stator diameter is directly derived from the value of the nominal power. But if the available installation space is limited and the outer dimensions are fixed, the approach must be different. In this paper the machine's optimal rotor diameter and pole-pair number are first determined by analytical considerations and numerical calculations regarding the requirements depending on the drive-cycle simulations of the parallel vehicle. In a second step this initial geometry of the electrical machine is optimized by means of numerical simulations. Among others the rotor diameter, pole pitch, magnet height, tooth width, yoke height, addendum and the tooth tip width are optimized in order to improve the power density, the overload capacity, the torque ripple and the overall efficiency.

References

[1] M. Zeraoulia, M.E.H. Benbouzid, D. Diallo. "Electric Motor Drive Selection Issues for HEV Propulsion Systems: A Comparative Study", *IEEE Trans. on Vehicular Technology*, Vol.55, No.6, November 2006.

[2] L. Chang. "Comparison of AC Drives for Electric Vehicles - A Report on Experts' Opinion Survey", *IEEE AES Systems Magazine*, August 1994.

[3] M. Yabumoto, C. Kaido, T. Wakisaka, T. Kubota, N. Suzuki. "Electrical Steel Sheet for Traction Motors of Hybrid/Electrical Vehicles", *Nippon Steel Technical Report*, No.87, July 2003.

[4] J.G.W. West. "Propulsion systems for hybrid electric vehicles", *Electrical Machine Design for Electric and Hybrid-Electric Vehicles, IEE Colloquium on*, pp. 1/1 - 1/9, October 1999.

[5] C.C. Chan. "An overview of electric vehicle technology", *Proceedings of the IEEE*, Volume 81, Issue 9, Page(s):1202 - 1213, September 1993.

[6] Thomas Finken, Matthias Felden, Kay Hameyer. "Comparison and design of different electrical machine types regarding their applicability in hybrid electrical vehicles", *Proceedings of the ICEM*, September 2008.

[7] BMWi, TÜV Rheinland. "Europa Hybrid - Innovativer PKW-Hybridantrieb für Europa." Internet: http://www.tuvpt.de/newsletter/12007/neue-projekte.html, Jan. 2007 [Nov. 5, 2008].

[8] J. F. Gieras and M. Wing. *Permanent Magnet Motor Technology.* CRC, 2002.

[9] D. C. Hanselman. *Brushless Permanent Magnet Motor Design.* The Writers' Collective, 2003.

[10] G. Bertotti. "General properties of power losses in soft ferromagnetic materials", *IEEE Transactions on Magnetics*, Vol. 24, Issue. 1 pp. 621-630, January 1988.

[11] G. Bertotti, A. Boglietti, M. Chiampi, D. Chiarabaglio, F. Fiorillo, M. Lazzari. "An improved estimation of iron losses in rotating electrical machines", *IEEE Transactions on Magnetics*, Vol. 27, Issue. 6, pp. 5007-5009, November 1991.

[12] S. Domack. "Auslegung und Optimierung von permanenterregten Synchronmaschinen mittels Steuerverfahren und der Methode der finiten Elemente." PhD-thesis, RWTH Aachen, IEM, Verlag Shaker, Germany, July 1994.

[13] K.-C. Kim, D.-H. Koo, J.-P. Hong, J. Lee. "A Study on the Characteristics Due to Pole-Arc to Pole-Pitch Ratio and Saliency to Improve Torque Performance of IPMSM", *IEEE Transactions on Magnetics*, Vol. 43, No.6, pp. 2516-2518 , June 2007.